Inverse Lithography Technology Principles in Practice: Unintuitive Patterns

Yong Liu, Dan Abrams, Linyong Pang, Andrew Moore

Luminescent Technologies, Inc., 650 Castro Street, Suite 220, Mountain View, CA 94041

Email: yliu@luminescent.com

ABSTRACT

In this paper we present unintuitive patterns generated by inverse lithography technology. We show examples of contact hole masks designed with ILT that enjoy larger process windows than OPC. We also show variations in ILT-generated masks as the pitch of the contact hole array changes. In another example, we show poly masks designed for better process window to be substantially different from poly masks designed for better fidelity at nominal exposure-defocus (ED) condition. The mask with better fidelity has broken lines in comparison to the original layout. In a third example, we show deep trench mask patterns designed with ILT that, at first glance, bear no resemblance to the original layout, yet provide high fidelity in optical images. These patterns, although complex at first sight, can be generated in substantially simpler form with proper constraints without losing the spirit of ILT masks.

KEYWORDS: Inverse Lithography Technology (ILT), OPC, RET, Lithography

INTRODUCTION

Resolution Enhancement Technologies (RET) are widely used to cope with the severe optical effects that are manifest in semiconductor lithography. One of these technologies, optical proximity correction (OPC), requires ever expanding teams of engineers writing recipes for each class of basic layout topologies for each particular layer. These recipes dictate how the correction should be done for a layout topology in a varying environment. The recipes are based on applications of heuristics obtained from the human experiences of the teams of engineers. Some of these corrections are very clever, but they are not universal. Starting from 90nm, it has become more and more common that the best masks for printing the desired image patterns on wafers are beyond simple intuition.

Over the past 25 years, several physicists, mathematicians, and engineers have formulated the mask design problem in a different way, by considering it as an inverse problem and computing the required mask using entire area of the design pattern instead of just its edges [1-8]. This body of work may be described concisely as Inverse Lithography Technology (ILT). In this paper, we apply a new implementation of ILT to find mask patterns for contemporary semiconductor design patterns. Compared with edge-constrained OPC, ILT can compute whole-image solutions that may be non-obvious.

The implementation of ILT used considers several manufacturability constraints in formulating the inverse problem to be solved, for example: pattern fidelity at various exposure/defocus (ED) points including nominal (lithographic constraints); process window size and/or mask complexity (manufacturability constraints). By emphasizing either the pattern fidelity under nominal ED conditions, or the size of the process window, with the constraints and costs of mask manufacturing, and other lithographic objectives, one can automatically generate various mask patterns suiting different needs. The resulting masks have either high fidelity at nominal conditions or substantially improved depth-of-focus and exposure latitude, enabling printing of geometries that may otherwise be unattainable. We show contact-hole, poly and deep trench patterns that demonstrate both intuitive and unintuitive results obtained through the practice of ILT.

ILT APPROACH COMPARED WITH OPC

Lithography simulation is very time-consuming. To make OPC feasible for full chips, the design layout is first fragmented into segments. Based on the topology of the layout design, the segments may be long or short depending on the environment. On each segment, one (usually) or more sampling points are selected for image calculation. From the computed intensity on these sampling points, figures of merit for the whole area is inferred. The positions of these segments are modified to correct the deficiencies of the image (at those sampling points only). These corrections are carried out iteratively until satisfactory image qualities are achieved at all the sampling points. Some observations may be made regarding this computational approach. (1) The solution of this approach is a local one. This is so because the initial mask is very specific and the edge movement is local. Therefore any solution that represents large deviations from the initial layout is un-attainable from this approach. (2) Side-lobes and runny-noses are frequently undetectable by this approach since the number of sampling points is finite and intensities at other locations are ignored during OPC correction. (3) As a direct consequence of sparse sampling, post-OPC verification is required to check for both image quality and mask manufacturability. (4) Due to local nature of segment movement and the fact that numerous segments exist in a locality, the segment definition and sequence of segment movement will have a direct consequence on the final corrected image quality. Specific recipes for specific patterns are therefore needed to improve the quality and speed of OPC.

ILT, in contrast, considers the entire image when computing a mask pattern. As a direct consequence of this image-based approach, ILT has the following characteristics as compared to OPC. (1) All the image points are simultaneously accounted for during the inversion. (2) Side-lobes and runny-noses are detected and avoided during the mask computation. (3) As a direct consequence of image-based approach, image-quality-related post-OPC verification is not required since they are already accounted for during ILT mask computation. (4) No specific recipes to address specific patterns are required due to the image-based nature of ILT. (5) ILT can find mask solutions which are unintuitive and do not resemble the target pattern.

CONTACT HOLE ARRAYS

Contact hole arrays with Critical Dimensions (CD) of 113nm and array pitches varying from 200nm to 900nm were studied, with 193nm illumination. OPC, as represented by a simple bias, was imaged with six percent attenuated phase-shift mask technology. In contrast, chrome-on-glass mask technology was employed for ILT imaging in order to show its capabilities. Illumination conditions were optimized for simple bias and for ILT separately. The optimal parameters for simple bias are: numerical aperture of 0.6 and annular illumination with inner and outer radii of 0.6 and 0.9. The optimal illumination conditions for ILT are: numerical aperture of 0.78 and disk illumination with sigma of 0.3. The depth of focus (DOF) at 7% exposure latitude is plotted in Figure 1 against pitch for the two preparations.

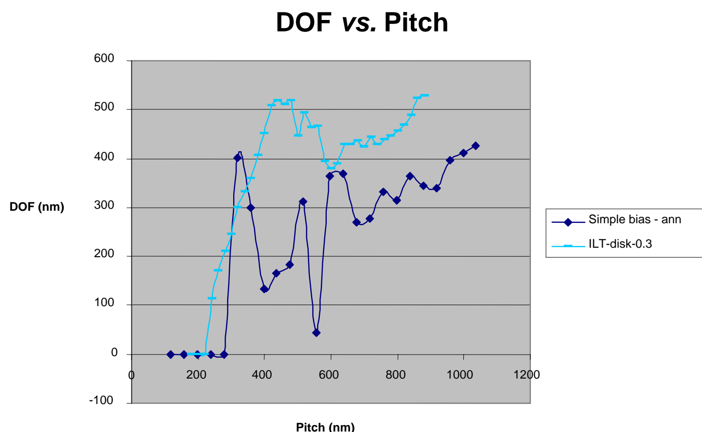

Figure 1. DOF of contact arrays at different pitches for both simple-bias masks and ILT masks at 7% exposure latitude.

As shown in Figure 1, the DOF of the ILT masks are on average 30-50% larger than that of simple-bias masks for this series of designs, despite the higher numerical aperture used for ILT. As a direct consequence, ILT masks can also resolve features at finer pitches than simple-bias OPC can. The single point in this series at which the simple-bias method has the larger DOF can be explained by the ringing effects of annular illumination. The pitch at this point is around two times wavelength, making resonance strong, especially for uniform contact-hole arrays. Except for this point, ILT-computed masks for this series achieve superior DOF even for more affordable and reliable binary mask technology.

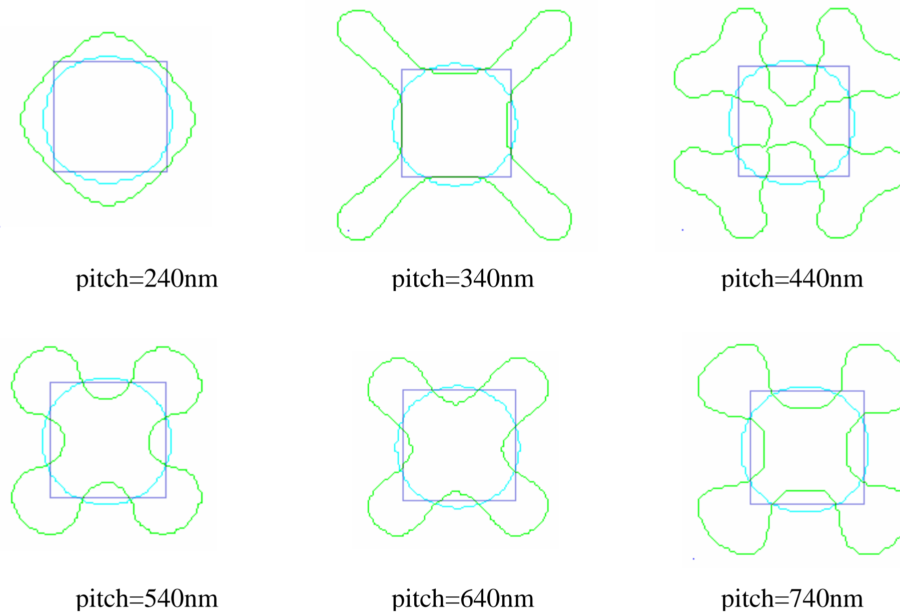

Figure 2. ILT mask pattern (green), target (blue) and image contour (aqua) for different pitches: 240nm, 340nm, 440nm, 540nm, 640nm and 740nm.

Figure 2 shows how the contact-hole ILT mask changes with pitch. When pitch is small, there is little room in between contact holes to allow mask serifs without the danger of image bridging between neighboring contact holes. Hence, the mask takes a diamond shape for pitch of 240nm. As pitches increases, this implementation of inverse lithography technology employs serifs to enhance the brightness of the hole image while minimizing interaction among neighboring contact holes. That is why the serifs are added at corners rather than at the centers of target edges. The particular shapes of the serifs vary with pitch, which to a large extent, determines how neighboring contact holes in the array optically interfere with one another.

These varying mask patterns with pitch can present significant difficulty to rule-based or recipe-based OPC when applied to random contact hole patterns. In contrast, these varying conditions are naturally handled by ILT, since ILT does not require any rules or recipes from the user.

POLYSILICON PATTERN

In the implementation of inverse lithography under study, it is possible to set up the inversion in various ways to achieve specific goals. The mask image may be computed as an inverse of the design pattern, with constraints on image quality at one or more ED points, including nominal. To achieve a goal of high fidelity at nominal ED, that point is

strongly weighted; to achieve a goal of large process window, ED points other than nominal are given more weight. In this section, we present an example of this with a poly pattern. The layout pattern is shown in Figure 3. The minimum poly feature size is 80nm and the minimum spacing is 100nm. A clear-field attenuated phase-shift mask was used with 193nm illumination, a numerical aperture of 0.85, and an annular light source of inner and outer radii of 0.5 and 0.85, respectively.

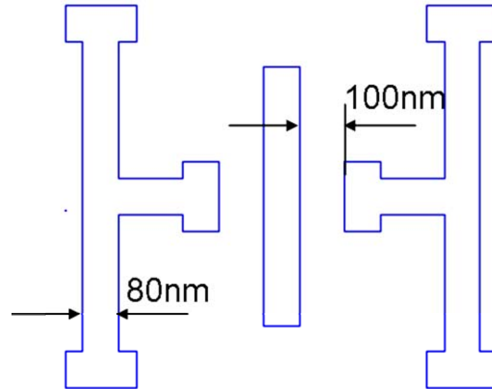

Figure 3. Sample poly layout pattern to compare inversion for better fidelity and for better process window.

In Figure 4, two masks computed by ILT with differing goals are shown. The one on the left (a) is designed for better fidelity at nominal ED. As one may observe, the mask pattern is quite curved with some dog-bone-like structures. At the location of the inner corners of the T structures in the original layout, the mask patterns are broken (disconnected) as compared to the layout. This broken structure is mostly due to the demand of maximum fidelity and the assumption that the photo-resist behavior mimics a threshold operation. To the extent that the photo-resist behavior closely approximates a threshold operation, the broken structure has real value in practice since some semiconductor devices are differentiated on speed/performance rather than cost. The high fidelity achieved through these structures results in narrower spread of device speed/performance, hence making it possible to target for more parts with high speed/performance.

On the right (b) of Figure 4 is ILT mask designed for better process window. This mask is less dog-bone-like, there is no broken structure, and the thickest and thinnest parts of Figure 4 (b) are different from those in Figure 4 (a). Clearly there are strong optical trade-offs between imaging for fidelity at nominal conditions and for a broad process window, and interference amongst parts of the curved ILT masks greatly impacts the mask result. This solution is less attainable in a rule- or recipe-based approach.

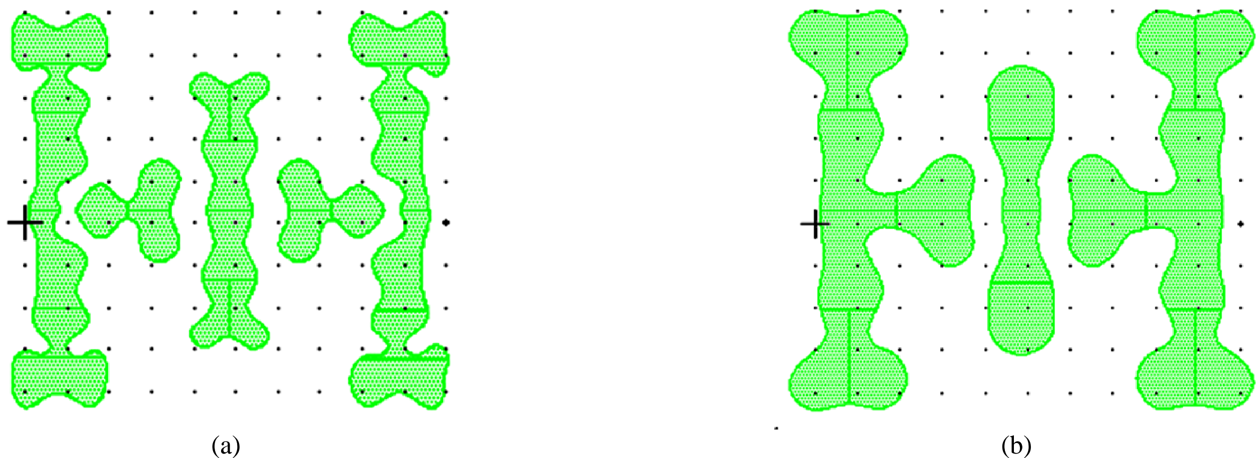

(a) (b)

Figure 4. Mask patterns for the poly layout of Figure 3, designed for better fidelity at nominal conditions (a) and for better process window (b).

Figure 5 shows image contours overlaid on the original layout for the masks in Figure 4. The contour image (red) of Figure 5a corresponds to the mask of Figure 4a. The contour image (red) conforms very well with the original layout (blue), indicating that ILT has achieved its objective of high fidelity at nominal ED. The broken masks resulted in continuous image lines with sharp corners. The contour images of Figure 5b correspond to the mask pattern of Figure 4b. Three contour images are shown (see inset of Figure 5b). The red contour is the computed forward image at nominal ED, the blue contour is the computed forward image at nominal focus and 7% dose variation, and the gray contour is the computed forward image at nominal exposure and 100nm defocus. As can be seen, the three contours do not comply exactly with the T corners, but in general they comply with the full design pattern very well, indicating good process window across the full design pattern.

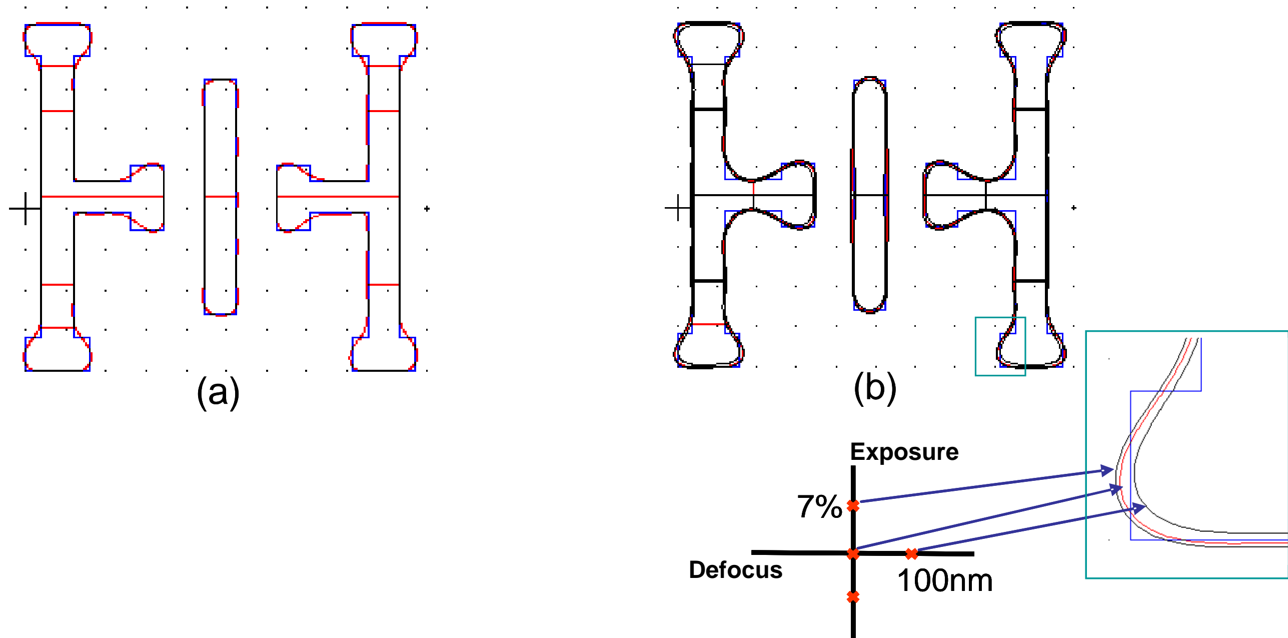

Figure 5. (a) Contour images (red) overlaid with original layout (blue) for the masks in Figure 4 (a). (b) Contour images at nominal exposure and focus (red), nominal focus and 7% exposure variation (light blue), nominal exposure and 100nm defocus (gray) overlaid with original layout (blue) for the mask in Figure 4(b). A zoomed-in set of contour image are shown in the inset.

DEEP TRENCH PATTERN

In this section, we show an ILT-computed mask for a deep trench design in which the mask pattern drastically differs from the original layout. Figure 6a shows one period of the design trench pattern. (The full pattern is a repetition of this pattern in both x and y directions.) The trench size is 135nm by 210nm, and the trench pitch is 200nm. A dark-field attenuated phase-shift mask was used with 193nm illumination, a numerical aperture of 0.7, and an annular light source with inner and outer radii of 0.57 and 0.85, respectively.

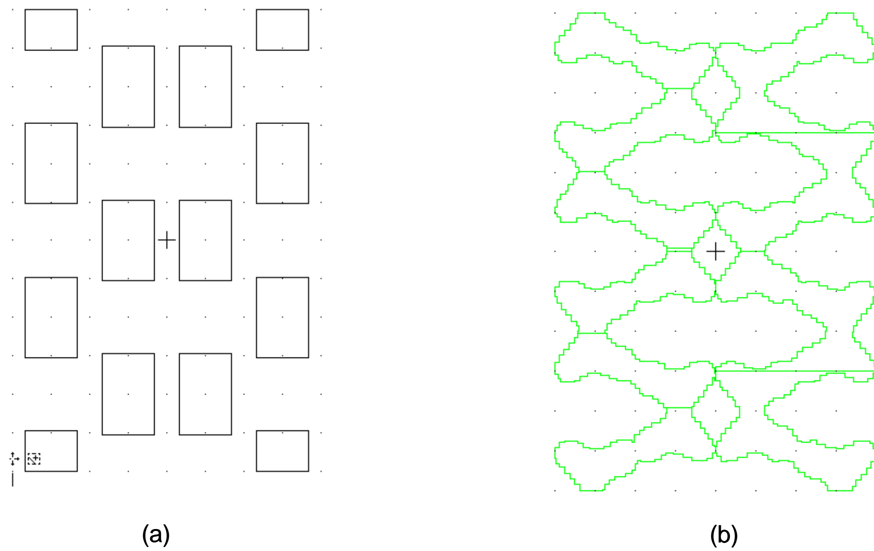

Figure 6. (a) Design layout of a deep trench pattern. The trench size is 135nm by 210nm. (b) ILT-computed mask pattern for the layout in (a), weighted for fidelity at the nominal exposure-defocus condition.

Figure 6b shows the mask computed using ILT, constrained for fidelity at nominal ED. At first glance, the mask pattern bears little resemblance to the design layout. Such a mask result is non-intuitive, and unlikely to be pre-programmed in a recipe for a traditional OPC approach. Upon closer inspection, one observes that it is an array of X-shaped patterns for each trench, with serifs extending so as to merge.

As shown in Figure 7, the contour images are not merged at the locations of the merged serifs. Furthermore, the contour images consist of good rectangular shapes rather than "peanut" shapes frequently seen for deep trench imaging.

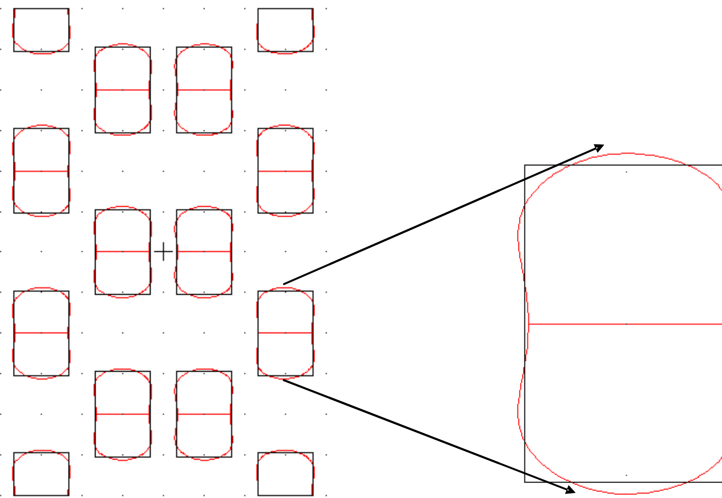

Figure 7. Image contour (red) at nominal conditions resulting from the ILT mask in Figure 6b, overlaid with the design layout (black).

The mask in Figure 6b has many small fracture sizes. This can result in large data volume and hence long mask write time and relatively high mask cost. To reduce data volume, one can specify minimum fracture constraints in the implementation of ILT used in this study. The resulting mask patterns still keep the spirit of ILT but are much simpler. The simpler mask patterns are shown in Figure 8 with fractured results shown at minimum mask edge length of 10nm, 30nm and 50nm.

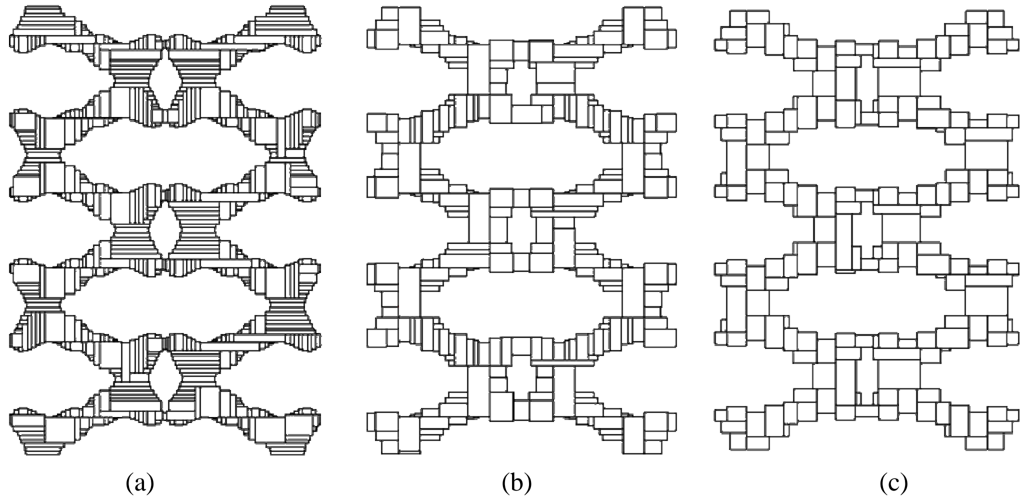

Figure 8. Fractured ILT-computed mask patterns for minimum fracture sizes of (a) 10nm, (b) 30nm and (c) 50nm for the layout of Figure 6a.

Mask figure counts are plotted in Figure 9 for two kinds of VSB machines and one kind of MEBES machine. This chart shows that the MEBES format has a smaller data volume than the VSB format for these masks, indicating– for his case at least – that a laser writer is more efficient at writing ILT masks than e-beam writers. The data volume at the 50nm minimum length is about 1.2 times that of OPC. The data volume at 30nm does not differ significantly from the data volume at 50nm, but it is about half of the data volume at 10nm. Therefore, the data volume at 30nm minimum edge length is likely acceptable given that the ILT-computed mask provides better image quality.

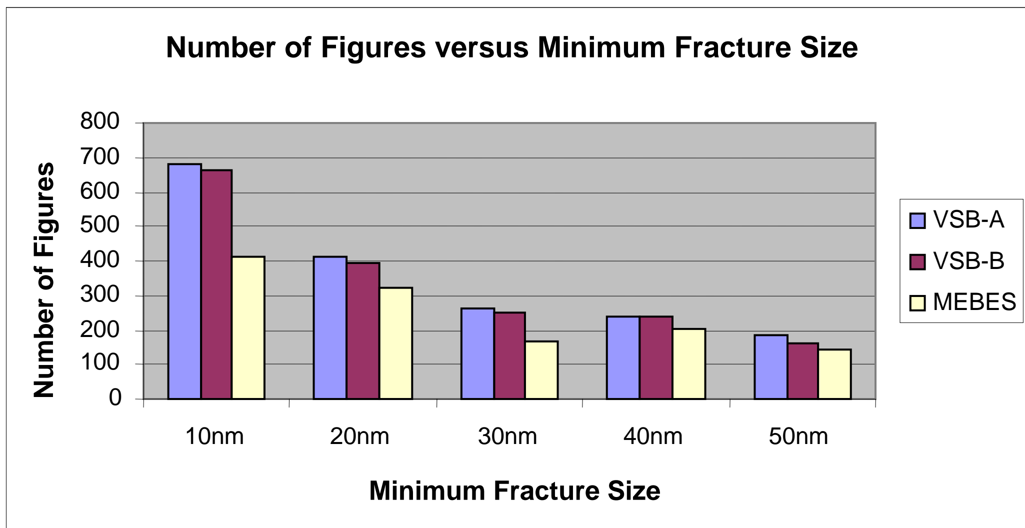

Figure 9. Figure count of ILT-computed masks with varying fracture size for the layout pattern of Figure 6a.

SUMMARY

Inverse lithography technology can be used to design masks with better fidelity at the nominal condition or with a better overall process window. The approach is image-based and hence image verification is built in. No damaging side-lobes printing should be expected from images of ILT masks. The ILT solutions are not local solutions like those found with OPC. Hence unintuitive mask patterns may be automatically generated without requiring an expert to write specific recipes as in OPC. ILT masks can be complex or simple depending on the constraints specified. One may trade-off image quality and mask complexities with ILT. With minimum fracture size of 50nm, ILT mask fractured data volume is in about the same range as conventional OPC.

ACKNOWLEGEMENTS

The authors would like to thank the whole Luminescent team for creation of the ILT implementation that made this work possible, and in particular to Danping Peng, Peter Hu and Gordon Russell for their help in some of the test cases. The authors also wish to thank Becky Tsao and Promos Technologies for support of this work.

REFERENCES

1. B.E.A. Saleh and S.I. Sayegh, Reductions of errors of microphotographic reproductions by optical corrections of original masks, Optical Eng. Vol. 20 pp 781-784 (1981)
2. K.M. Nashold and B.E.A. Saleh, Image construction through diffraction-limited high-contrast imaging systems: an iterative approach, J. Opt. Soc. Am. A, vol. 2 p. 635 (1985)
3. Y. Liu and A. Zakhor, Optimal binary image design for optical lithography, Proc. SPIE Vol. 1264 pp 410-412 (1990)
4. Y. Liu and A. Zakhor, Binary and phase-shifting image design for optical lithography, Proc. SPIE Vol. 1463 pp 382-399 (1991)
5. Y-T Wang, Y.C. Pati, H. Watanabe and T. Kailath, Automated design of halftoned double-exposure phase-shifting masks, Proc. SPIE Vol. 2440 pp 290-301 (1995)
6. S-H Jang et. al, Manufacturability evaluation of model-based OPC masks, Proc. SPIE vol. 4889 p 520 (2002)
7. A. Rosenbluth et. al, Optimum mask and source patterns to print a given shape, JM3 vol. 1 pp 13-30 (2002)
8. T. Fuhner and A.Erdmann, Improved mask and source representations for automatic optimization of lithographic process conditions using a genetic algorithm, Proc. SPIE Vol. 5754 pp 415-426 (2005)